



African Journal of Biological Sciences



An In-Vitro Investigation Contrasting the Ability of Cone Beam Computed Tomography and Digital Intraoral Bitewing Radiography to Detect Periodontal Defects

Ahmed Aasy^{1*}, Gehan G. El-Desouky², Wael S. Amer²

^{1*} Department of Oral radiology, October 6th University, Giza, Egypt

² Department of Oral and Maxillofacial Radiology, Faculty of Dentistry, Suez Canal University, Ismailia, EGY

* Corresponding author

e-mail: ahmed.hussein.dent@o6u.edu.eg

Tel: +201068233328

Abstract:

Introduction:Chronic periodontitis affects the periodontium of adult population.The assessment of bone loss in chronic periodontitis requires comprehensive clinical and radiographic examinations. Bitewing radiographs can provide vital information about the amount of alveolar bone loss.However, drawbacks of 2D imaging like superimposition and distortion can hamper diagnosis. Cone Beam Computed Tomography (CBCT) has improved the diagnosis of various conditions in the maxillofacial region with its superior diagnostic ability. **Aim:** The aim of our study was to compare the accuracy, reliability, and diagnostic abilities of standard resolution CBCT and intra-oral Digital Bitewings in the assessment of periodontal defects compared to physical measures. **Materials and methods:** Different patterns and sizes were created on eight dry human skulls simulating periodontal defects. The created defects were scanned with standard resolution CBCT and intraoral digital bitewing to compare reliability, diagnostic accuracy, and detectability of both protocols. **Results:**Standard resolution CBCT and digital intraoral bitewing showed statistically higher values compared to the physical measurements regarding smaller-sized intra-bony defects (1-2 mm) and a non-significant difference in larger-sized defects (3-4 mm), when compared to the gold standard ($p < 0.05$). Additionally, bitewings were unable to detect dehiscence and fenestration.**Conclusion:** When investigating large interproximal defects, standard resolution CBCT and bitewing radiographs can show similar results in terms of accuracy and detectability. When surface defects are expected, CBCT is recommended as the diagnostic modality of choice. Nevertheless, CBCT should not be the primary imaging technique of choice for periodontal evaluation.

Keywords: Periodontitis,intra-bony defects, CBCT, Bitewing.

Article History

Volume 6, Issue 5, 2024

Received: 15 May 2024

Accepted: 02 Jun 2024

doi: 10.48047/AFJBS.6.5.2024.9442-9460

Introduction

Periodontitis is a multifactorial, microbially associated, host-mediated chronic inflammatory disease characterized by progressive destruction of the periodontal attachment apparatus. Loss of periodontal tissue support is the primary feature of periodontitis, which is observed by circumferential clinical assessment of fully erupted teeth using a standardized periodontal probe with reference to the cemento-enamel junction (Raindi 2015, López et al., 2016 and Jack et al., 2018).

Progression of periodontitis can lead to alveolar bone loss, which may be present in the form of intra-bony defects like infra-bony pocket, which is a deepening of the gingival sulcus where the base of the pocket is at lower level than that of the alveolar bone (Weinberg et al., 2000 and Trombelli et al., 2018), and supra-bony defects like dehiscence, which is a V-shaped superficial defect which occurs at the crestal margin of the alveolar bone and pointing towards the tooth apex (Leung et al., 2010) and fenestration, which is a circumferential, nearly rounded area at the tooth apical one third where the root has completely lost its alveolar bone coverage and is covered with periosteum (Nimigeon et al., 2009 and Wong 2021).

Alveolar bone loss in periodontitis and the subsequent formation of different alveolar bone defects (Zhang et al., 2021), can go undiagnosed in routine clinical examination. The use of adjuvant diagnostic methods, like x-rays, can greatly contribute to the assessment of periodontal status (Eke et al., 2000 and Huang 2020).

Radiographic imaging methods used for clinical evaluation and treatment are crucial for diagnosis and prognosis of periodontal disease. Intraoral bitewing and Cone Beam Computed Tomography (CBCT) imaging x-rays are two different types of radiographic examinations that

can be used for the detection of periodontal problems. CBCT imaging provides three-dimensional(3D) multi-planer images in three orthogonal planes (sagittal, coronal and axial)for the teeth and surrounding structures, free from superimposition and distortion, while intraoral bitewing x-rays provide two-dimensional (2D) images of mainly interproximal alveolar bone(Asiri et al., 2020 and Khanna 2020).

Intraoral bitewing x-rays are still considered the standard of care for most cases of periodontal disease, especially when expecting the presence of infra-bonyperiodontal pockets,while CBCT imaging may be indicated for more complex or advanced cases that require more detailed information(Sousa et al., 2020).However, theparticular use of each modality in different clinical situations and the guidelines for modalities selectionare still questionable.Therefore, the aim of this study was to compare the reliability, accuracy, and detectability of standard resolution CBCT and intraoral bitewing radiographs inthe detection of different periodontal defects.

Materials and Methods

Study setting:

The present research was conducted at Oral and Maxillo-facial Radiology Department, Faculty of Dentistry, Suez Canal University, on eight dry human skulls of unknown age, sex or ethnicity, on which periodontal defects were created resembling the infra-bony defect, dehiscence and fenestration, and scanned with intraoral digital Bitewings and standard resolution CBCT. Skulls were obtained from the Human Anatomy Department, Faculty of Medicine, Cairo University.

Sample size calculations:

The aim of this study was to compare the accuracy, reliability, and diagnostic abilities of standard resolution CBCT and intra-oral Digital Bitewing imaging in the assessment of alveolar bone loss compared to real physical measures. Accordingly, a minimum total sample size of eight skulls was sufficient to detect an effect size of 0.46 and a power of 80% at a partial eta square of 0.18. The sample size was calculated using G*power version 3.1.9.6 for Mac OS (figure 1)(Cohen et al., 1988, Faul et al., 2007 and Faul et al., 2013).

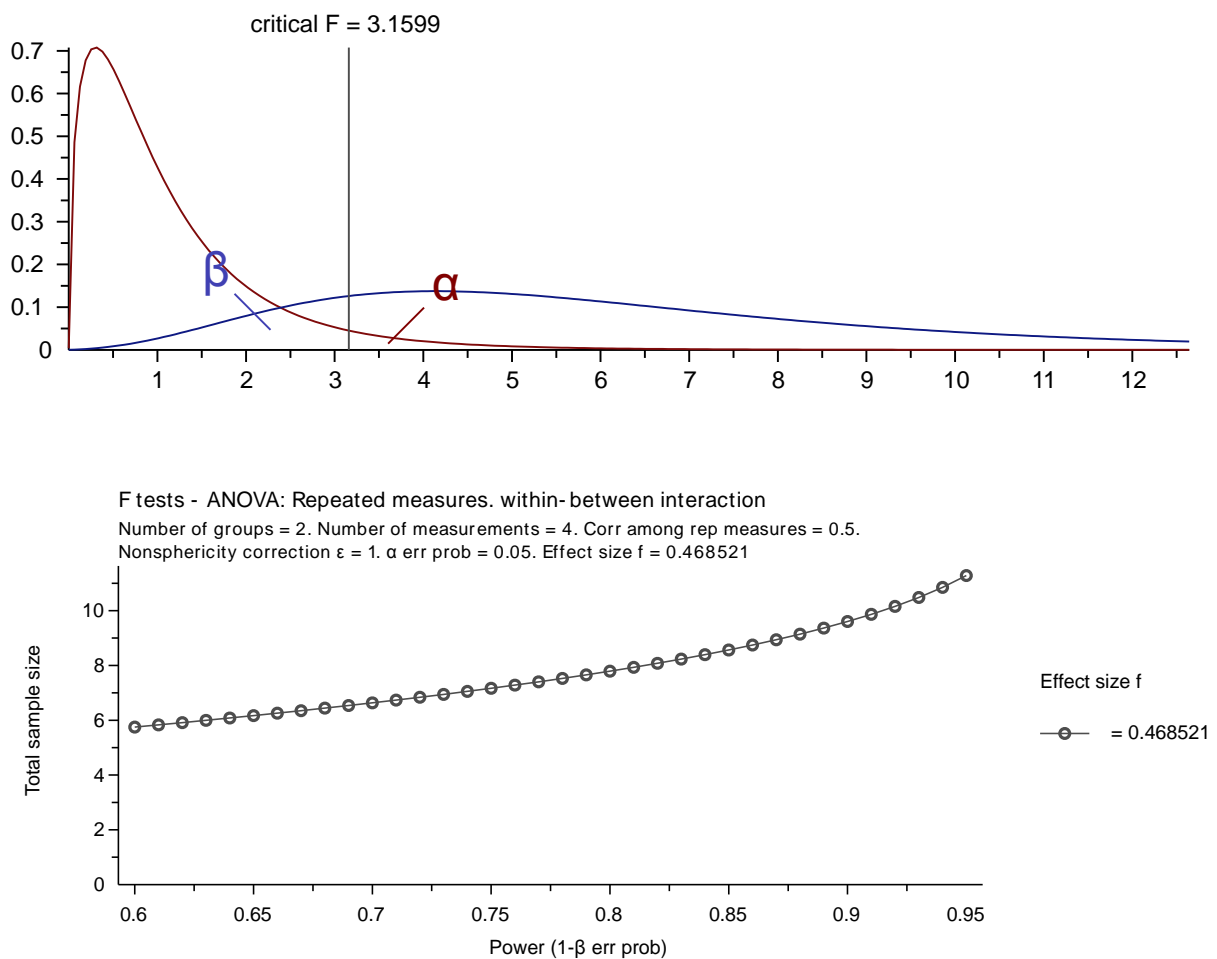


Figure 1. sample size calculations, power versus sample size and probability plot.

Sample selection and creation of periodontal defects:

The present study was conducted on eight dry human skulls, of unknown age, sex, or ethnicity. Skulls were included in the current study based on the following criteria:-fully or partially dentated -with no metal fillings or appliances -no pre-existing periodontal defects or conditions which may affect the integrity and shape of the alveolar bone.

On the eight skulls, a total number of 79 defects were created. The defects were distributed 33 in the maxillae and 46 in the mandibles and were created on the available sound alveolar bone of the jaws in each skull. Nine defects were created in the anterior area, 20 defects were created in the premolar area, while 50 were created in the molar area (either maxillary or mandibular).

The defects were created using a low-speed handpiece and a micro-motor of 800 rpm with round diamond burs of different sizes to make different defect types (infra-bony defects, dehiscences and fenestrations) with different sizes (1, 2, 3 and 4mm).

The 79 defects were created resembling different common periodontal conditions as follows:

- **Intra Bony pocket (IBP)** was created starting from the proximal surface of the tooth at the crest of the alveolar bone proceeding in an apical direction within the body of alveolar bone tangent to the root of the involved tooth creating a total number of 31 IBP (Leung et al., 2010).
- **Fenestration** was created at the level of the apical part of the root using round diamond bur at the center of the root on the facial alveolar bone (labial / buccal) and extending circumferentially. Fenestrations were created only on the buccal and labial surfaces of the

maxillae and mandibles of the dry skulls creating a total of 16 fenestration defects (Caton et al., 1999).

- **Dehiscence** was created on the labial, buccal, lingual, and palatal surfaces of the maxillae and the mandibles of the dry skulls creating a total number of 32 dehiscences. The dehiscence was created starting from the alveolar crest and proceeding in an apical direction but this time the defects were created in a superficial pattern where the inner wall of the defect was the root of the involved tooth (Leung et al., 2010).

The dimensions of the created defects were measured twice with two weeks intervals using a digital caliper of 0.1mm accuracy, the mean of the two readings was assigned as the gold standard.

Ten layers of pink wax each of 1.5 thickness (Total thickness of 15mm) were then applied to the facial surface of the skulls starting from the infraorbital rim to the lower border of the mandible to simulate the thickness of soft tissues coverage in those areas, to mimic the clinical exposure conditions and attenuation factors for the human head according to the guidelines of Richard *et al.*, (2005).

Radiographic examination and assessment:

Intra-oral digital bitewing examination: skulls were subjected to digital intraoral bitewing x-ray examination (Acteon X-Ray X-Mind Dc. focal spot 0.4, 60-70 kVp, 7mA, exposure time 0.6s) using a size 2 Photostimulable Phosphor (PSP) plate, and a bitewing XCP (Extension Cone Parallel) film holder to scan the created defects in each jaw of the skulls. The measurements for IBD were carried out using linear measurement tool in Digora software (DIGORA 2.5. Soredex, Tuusula, Finland) on a personal computer, starting at the cemento-enamel junction of the involved tooth tangent to the root surface till the deepest visible point of the created defect.

CBCT examination: The skulls were scanned with standard resolution, with the scanner set at XL FOV (80x165-mm), 10 mA, 90 kV for a single scan of 360° rotation and total scan time of 2.4 sec, with voxel sizes of 0.4mm and total exposure of 856 mGycm². The CBCT scanner used in the present study was Scanora 3dx (Scanora 3D, Finland, Helsinki™, KVp: 60-90, mA: 4-10, scan time: 2.4-6, focal spot: 0.5. Detector: Flat panel a-Si. Voxel size: 0.4mm).

All the defects in each skull from the standard protocol CBCT scan were detected radiographically, measured, and recorded. Detection of defects and measurement of their dimensions was performed on a personal computer using On-Demand software using ruler tool for linear measurements. For intra-bony defects, CBCT measurements were made on sagittal cuts starting at the crest of the alveolar bone till the deepest point of the pocket (figure 2.a) while bitewing measurements were carried out starting at the crest of the alveolar bone till the deepest visible point of the pocket base (figure 2.b). For dehiscence, measurements were made on volume rendered (VR) view between edges of the defect tangent to the apical root surface (figure 3.a). Fenestration measurements were also made on VR view to measure if the diameter of the



fully made circular defect was tangent to the apical root surface (figure 3.b).

Figure (2): Linear measurement for infra-bony defect(a). Standard resolution CBCT from On-Demand software on sagittal view (b). Digital intraoral bitewing from Digora software.

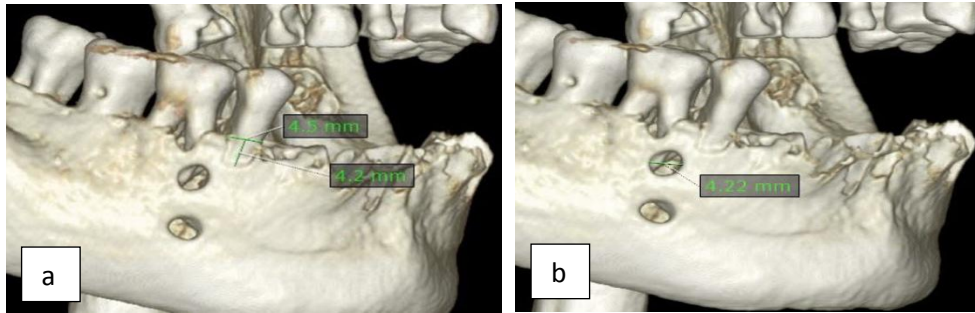


Figure (3): Linear measurement on volume rendered windows from On-Demand software (a). Standard resolution CBCT for dehiscence defect (b). Standard resolution CBCT from On-Demand software for fenestration defects.

Measurements from standard resolution CBCT and intraoral bitewing scans as well as the real physical measurements were made once and repeated two weeks later by the same observer for intra-observer reliability assessment.

Statistical Analysis

In the present study, the radiographic measurements of created defects (infra-bony defect, dehiscence and fenestration) obtained from standard CBCT resolutions and digital intraoral bitewing radiographs were compared to the actual clinical measures obtained by the digital caliper. The collected numerical data was summarized using means and standard deviations. The recorded data was then tabulated for statistical analysis.

In the current study, Cronbach's alpha and interclass coefficient (ICC) analysis were used to measure internal consistency between intra-observer records, to determine how close they were related.

To state whether the recorded data was significant or non-significant, an ANOVA test was used. Since it allows a comparison of more than two groups at the same time to determine whether a relationship exists between them or not.

In this study comparisons between linear actual measurements (gold standard) and radiographic measurements were made using the independent Duncan's Multiple Range Test (DMRT). All p-values were two-sided (estimated values may be more than or less than the reference value). P-values ≤ 0.05 were considered significant.

Results

A total number of 79 defects (infra-bony defect, dehiscence and fenestration) were created in the alveolar processes of 8 human dry skulls. Real physical measures were obtained using a digital caliper and considered the gold standard for this study. The skulls were then radiographically scanned to obtain standard resolution CBCT (voxel size 0.4mm) and intraoral bitewing radiographing images. The obtained measurements from both protocols were recorded and assessed.

Reliability test performed for analysis of both readings of the one operator twice showed very close intra-observer agreement varying from 0.922 to 1.00 for all readings obtained for the gold standard physical measurements, standard resolution CBCT and digital bitewing scans using Cronbach's alpha and interclass coefficient (ICC) analysis.

Table (1) presents the mean and standard deviation (SD) values and comparison between the physical measures "gold standard" and standard resolution CBCT and bitewing images for the infra-bony defects (IBDs) created with different sizes. For the infra-bony defects (IBD) size 1mm and 2mm measurements, the mean values of both standard resolution CBCT and intraoral bitewings showed a statistically significant difference when compared to the mean value of the

gold standard ($p < 0.05$). On the other hand, for the infra-bony defects (IBD) size 3mm and 4mm, the mean values of both, standard resolution CBCT and intraoral bitewings showed a statistically non-significant difference when compared to the mean value of the gold standard ($p > 0.05$).

Table 1: Comparison between gold standard, standard resolution CBCT and bitewing images regarding the created IBDs.

| IBD | | | | |
|--------------------|----------------------|---------------------------------|-----------------------|----------------|
| Defect size | Gold standard | Standard resolution CBCT | Bitewing x-ray | p-value |
| 1mm | 1.13 ± 0.06^b | 1.33 ± 0.25^a | 1.34 ± 0.24^a | 0.007* |
| 2mm | 2.08 ± 0.14^b | 2.48 ± 0.18^a | 2.41 ± 0.19^a | <0.001** |
| 3mm | 3.23 ± 0.24^a | 3.26 ± 0.23^a | 3.39 ± 0.26^a | 0.432 ns |
| 4mm | 4.14 ± 0.13^a | 4.19 ± 0.15^a | 4.21 ± 0.15^a | 0.395 ns |

* ** : significant at $p < 0.05$, 0.01, 0.001; ns: non-significant at $p > 0.05$. Means followed by different letters (^{a/b}) in the same row (horizontally) are significantly different according to DMRTs at 0.05 level.

In the present study, regarding dehiscence and fenestration defects, for their nature being surface defects, dehiscence and fenestration were not detectable on intraoral bitewings, consequently their results were not eligible for comparison in this study. However, the dehiscence and fenestration data obtained from CBCT scans were compared to the direct physical measurements of the digital caliper.

Table (2) presents the mean and standard deviation and results of the comparison between the gold standard and the standard resolution CBCT for the created dehiscence defects, while table (3) presents the mean and standard deviation and results of the comparison between the gold and the standard resolution CBCT for the created fenestration defects.

Regarding the dehiscence and fenestration small-sized defects (1 and 2mm), standard resolution CBCT showed statistically significantly higher values when compared to the mean value of the gold standard ($p>0.05$). While in medium and larger defects for both dehiscence and fenestration (3 and 4mm), standard CBCT showed non-significant differences.

Table 2: Comparison between gold standard and standard resolution CBCT regarding the created dehiscence defects.

| Dehiscence | | | |
|--------------------|----------------------|---------------------------------|---------------------|
| Defect size | Gold standard | Standard resolution CBCT | p-value |
| 1mm | 1.19 ± 0.11^b | 1.48 ± 0.17^a | 0.005* |
| 2mm | 2.14 ± 0.16^b | 2.51 ± 0.12^a | <0.001** |
| 3mm | 3.15 ± 0.18^a | 3.2 ± 0.12^a | >0.05 ^{ns} |
| 4mm | 4.14 ± 0.14^a | 4.16 ± 0.16^a | >0.05 ^{ns} |

*, **: significant at $p<0.05$, 0.01, 0.001; ns: non-significant at $p>0.05$. Means followed by different letters (^{a/b}) in the same row (horizontally) are significantly different according to DMRTs at 0.05 level.

Table 3: Comparison between gold standard and standard resolution CBCT regarding the created fenestration defects of different sizes.

| Fenestration defect | | | |
|----------------------------|--------------------------|--------------------------------|---------------------|
| Defect size | Gold standard | Standard resolutionCBCT | p-Value |
| 1mm | 1.03 ± 0.05 ^b | 1.48 ± 0.16 ^a | >0.05 |
| 2mm | 2.07 ± 0.08 ^b | 2.31 ± 0.13 ^a | >0.05 |
| 3mm | 3.17 ± 0.14 ^a | 3.21 ± 0.13 ^a | <0.05 ^{ns} |
| 4mm | 4.04 ± 0.12 ^a | 4.1 ± 0.14 ^a | <0.05 ^{ns} |

* , ** : significant at p<0.05, 0.01, 0.001; ns: non-significant at p>0.05. Means followed by different letters (^{a/b}) in the same row (horizontally) are significantly different according to DMRTs at 0.05 level.

Discussion

Periodontitis is a chronic host-mediated inflammatory disease characterized by inflammation of the periodontium which leads to alveolar bone loss and subsequent loss of teeth. Early detection of periodontitis plays a great role for better treatment planning and post operative prognosis. Careful diagnosis using adjuvant aids like intra, and extra oral radiographic imaging can contribute to early detection and diagnosis of periodontitis. Intraoral digital bitewing images have been for long considered the gold standard for early detection of inter proximal alveolar bone loss in periodontitis. On the other hand, CBCT images provide high-quality three-dimensional images for small structures, free from superimposition and distortion (Zhao 2015 et al., and Zhang et al., 2020).

Therefore, the present study was performed to compare the accuracy, reliability and diagnostic abilities of standard resolution CBCT and intra-oral Digital Bitewing imaging in the assessment of alveolar bone loss compared to real physical measures.

The study was conducted on eight dry human skulls, partially or fully dentated adult, with no metallic filling or appliances, no existing conditions or abnormal anatomical variations in alveolar bone, no crowding to create periodontal defects with different sizes, sites and types.

In 2015 Zhao *and* his co-workers recommended that the skulls included in their study to be of adults, to ensure that the alveolar process is fully developed and with enough mineral content for convenient creation of the defects, proper examination, and optimum visualization on intra oral radiographs and CBCT images, hence the skulls used in the current study were chosen to be of adult's individuals.

The skulls included in the current study were with either partially or fully dentated jaws and with intact alveolar anatomy, to have sufficient alveolar bone structure for defects creation and simulation, since periodontitis occurs in about/around tooth structure. The integrity of the teeth roots was a must in the selection criteria of the skulls in our study, for the fact that the majority of the pathologic periodontal defect occur around the roots of the teeth since it is an essential part of the tooth involved with the progression of periodontitis. In addition, to ensure better contrast on radiographs and CBCT images.

Following the guidelines of Zhang *and* his team in 2020 careful examination of the skulls was performed to ensure that there was no present previous alveolar bone destruction, bony prominences or abnormalities that would change the density of the alveolar bone and subsequently affect the creation of the defects in a way that mimics their pathologically occurring counterparts. Normal alignment of the teeth without crowding facilitates the creation of the defects in the interproximal areas between the adjacent teeth and better detection of these defects on the 2D bitewing radiographs for comparison with CBCT images.

In the current study, dried skulls were selected without any metallic fillings, appliances, or metallic prosthetic parts to avoid any possible effect on the accuracy of measurements from CBCT images that may be the result due to metallic artifacts such as scatter and beam hardening. This was in accordance with the guidelines of Scarfe and Angelopoulos(2018) who stated that, the image data set can sometimes be utterly useless for diagnostic purposes when streak artifacts that arise from metallic objects obscure anatomical structures in the affected slices. Interfering with the clear visibility of structures in the vicinity of, or in between, metallic objects and hence could affect the accuracy of the linear measurements.

In the current study, the guides of Kamburoğlu and his team (2018) were followed to avoid the inaccuracies in the size and integrity of defect margins, in this study we used diamond round burs to produce sharper margins for better measurement recording and reading.

Many methods have been used to clinically and radiographically assess alveolar bone such as periodontal probes, manual and digital calipers, bitewing radiographs, periapical paralleling radiographs, conventional CT and cone beam computerized tomography (CBCT) (Scarfe and Angelopoulos 2018). Among such modalities, CBCT images show absence of distortion and overlapping, and image dimensions comparable with the actual size of the scanned objects. CBCT has been proven to show parallel accuracy when compared to direct measures obtained from digital caliper (Kamburoğlu et al., 2018 and Fokas et al., 2015). Therefore, CBCT was chosen in the present study to be the imaging modality for the assessment and detection of the periodontal defects in this study in comparison to digital bitewing radiographs.

Bitewing radiographs are routinely used for evaluation of interproximal alveolar bone loss and pocket depth assessment in periodontitis. In the current study, bitewing x-rays were used to compare the results with CBCT images, since it the most accurate type of intraoral

radiographs in terms of detection and assessment of the initial interproximal periodontal defects, as recommended by Cheng et al., 2016, Cetmili et al., 2019 and Sharma et al., 2019 and his team. For precise standardized intraoral imaging, in the current study bitewing radiographs were taken using paralleling cone technique with the help of extension cone paralleling (XCP) device (Chenget al., 2016).

Reliability analysis was performed for all measurements obtained in our study to assess the accuracy of the readings obtained by the observer at different time intervals. The results for intra-observer agreement in the current study showed firm agreement between the two observations (varying from 0.922 to 1.00 for both readings) which indicated the high reliability of the intra-observers records to be used for assessment.

Regarding the IBD, although there was a statistically significant difference between both imaging modalities and the gold standard, CBCT showed superior accuracy in relation to the gold standard for assessing the smaller lesions (1 and 2mm). While for the medium and large sized defects (3- 4mm) a statistically non-significant difference was recorded, and CBCT still showed superior accuracy for assessment of the IBD compared to the intraoral digital bitewings. However, with medium and large defects, the detectability of the defects was not of paramount difficulty between the two modalities. A finding which revealed that the detectability and the accuracy of the created defects increased with increase in size of the defect in both protocols.

Another study conducted by Bagis et al., (2015) on 12 dry skulls with maxilla and mandible to create artificial defects (dehiscence, tunnel, and fenestration) on anterior, premolar and molar teeth separately using burs. In total, 14 dehiscences, 13 fenestrations, 8 tunnels and 16 periodontal defects were created. They used standard resolution CBCT and bitewing intraoral

digital radiographs to scan the defects. They concluded that CBCT has the higher sensitivity and diagnostic accuracy for detecting various periodontal defects between both radiographic modalities used.

Song *et al.*, (2021) conducted a study on fifty-four mandible blocks with implants harvested from nine male healthy adult beagle dogs and scanned them using intraoral bitewing radiographs and CBCT, in comparison to micro-CT as the gold standard, to assess the diagnostic accuracy of CBCT and intraoral radiographs in evaluation of peri-implant defects. They concluded that the diagnostic accuracy and reliability of CBCT was superior to intraoral bitewing radiographs for the detection, classification, and measurement of peri-implant bone defects. Their results were not in line with the results of the current study except regarding the small sized defects.

Another study was conducted by Almeida *et al.*, (2017) who simulated interproximal periodontal defects using perchloric acid on twenty dry pig mandibles creating a total number of 80 experimental sites. They scanned the created defects with CBCT and intraoral bitewing radiographs and concluded that CBCT performance was not superior to that provided by intraoral radiographs. The results of their study were partly in line with our study for the large sized defects. The conflict in results can be explained on the basis of size of the created defects in the study of Almeida and his team. Since large interproximal defect sizes ≥ 4 mm are much easier to be detected and assessed on intraoral films.

Regarding dehiscence and fenestration, only CBCT images were capable of detecting and evaluating these defects. This result was in line with that of Vasconcelos and his colleagues (2012) who compared periapical radiographs and standard resolution CBCT for the detection of dehiscence and fenestration. They concluded that CBCT was the only method that

allowed for an analysis of the defects occurring on the buccal and lingual/palatal surfaces (dehiscence and fenestration) with an improved visualization of the morphology of these defects.

Conclusion

When investigating large interproximal infra-bony defects, standard resolution CBCT and intraoral bitewing radiographs can show similar results in terms of detectability, accuracy and assessment. When surface defects are expected, CBCT imaging should be the modality of choice. However, due to its high radiation dose, CBCT should not be used as the first modality for periodontal evaluation. When performing clinical periodontal examination and expecting the presence of surface defects like dehiscence and fenestration, CBCT should be the modality of choice for proper diagnosis, given that the surface defects cannot be detected using 2D modalities.

References

- Raindi D. Nutrition and Periodontal Disease. Dent. Update 2015; 43: 66–68.
- López SAF, Lin GH, Monje A, Galindo- Moreno P, & Wang HL. Influence of soft tissue thickness on peri- implant marginal bone loss: A systematic review and meta- analysis. *Journal of periodontology* 2016;87(6), 690-699.
- Jack C, Gary A, Tord B, Iain C, Søren J, Kenneth K, Brian M, Panos P, Mariano S, Maurizio T. A new classification scheme for periodontal and peri-implant diseases and conditions - Introduction and key changes from the 1999 classification. American Academy of Periodontol and European Federation of Periodontology. *J Periodontol* 2018;89 (Supp 1): S159-S172.
- Trombelli L, Farina R, Silva C O & Tatakis D N. Plaque- induced gingivitis: Case definition and diagnostic considerations. *J Clin Periodontol* 2018;45:44-67.
- Weinberg MA, & Eskow R N. Osseous defects: proper terminology revisited. *J Periodontol* 2000; 71(12): 1928.
- Leung CC, Palomo L, Griffith R, and Hans MG. Accuracy and reliability of cone-beam computed tomography for measuring alveolar bone height and detecting bony dehiscences and fenestrations. *Am J Orthod Dentofacial Orthop* 2010;137: S109-119.

- Nimigean VR, Nimigean V, Bencze MA, Poesina ND, Cergan RS and Moraru. Alveolar bone dehiscences and fenestrations:an anatomical study and review. Rom J MorpholEmbryol 2009;50(3):391–397.
- Wong J., Lee A., Zhang C. Diagnosis and Management of Apical Fenestrations Associated with Endodontic Diseases: A Literature Review. EurEndod J.2021;Apr;6(1):25-33. doi: 10.14744/eej.2020.51422.
- Zhang X, Li Y, Ge Z, Zhao H, Miao L, & Pan Y. The dimension and morphology of alveolar bone at maxillary anterior teeth in periodontitis: a retrospective analysis—using CBCT. Int J Oral Sci 2021;12(1): 4.
- Eke PI, Borgnakke WS, Genco RJ. Recent epidemiologic trends in periodontitis in the USA. Periodontol 2000 2020;82(1):257-67.
- Huang X, Xie M, Xie Y, Mei F, Lu X, Li X, & Chen L. The roles of osteocytes in alveolar bone destruction in periodontitis. J Transl Med. 2020;18(1): 479.
- Assiri H, Dawasaz AA, Alahmari A, & Asiri. Cone beam computed tomography (CBCT) in periodontal diseases: a Systematic review based on the efficacy model. BMC Oral Health 2020;20(1):191.
- Khanna AB. Applications of cone beam computed tomography in endodontics. *Evid.-based endod* 2020;5:1. <https://doi.org/10.1186/s41121-020-00020-4>.
- Sousa Melo SL, Rovaris K, Javaheri AM, & de Rezende BGL. Cone-beam computed tomography (CBCT) imaging for the assessment of periodontal disease. Curr Oral Health Rep 2020;7(4): 376–380.
- Cohen, J. Statistical power analysis for the behavioral sciences. Hillsdale, New Jersey: Lawrence Erlbaum Associates 1988.
- Faul, F., Erdfelder, E., Lang, AG. et al. G*Power 3: A flexible statistical power analysis program for the social, behavioral, and biomedical sciences Behavior Research Methods (2007) 39: 175. <https://doi.org/10.3758/BF03193146>.
- Faul, F., Erdfelder, E., Buchner, A., & Lang, A.-G. G*Power Version 3.1.7 [computer software]. 2013 Universität Kiel, Germany.
- Leung CC, Palomo L, Griffith R, and Hans MG. Accuracy and reliability of cone-beam computed tomography for measuring alveolar bone height and detecting bony dehiscences and fenestrations. Am J Orthod Dentofacial Orthop 2010;137: S109-119.
- Caton JG, Armitage G, Berglundh CIL, Jepsen S, Kornman KS & Tonetti MS. A new classification scheme for periodontal and peri- implant diseases and conditions— Introduction and key changes from the 1999 classification. J Periodontol 2018;89:S1-S8.
- Richard Y.H, Nojima K, Adams W.P Jr and Brown S.A. Analysis of Facial Skin Thickness: Defining the Relative Thickness Index.PlastReconstr Surg2005;115(6):1769-1773. doi 10.1097/01.prs.0000161682.63535.9b.

- Zhao H, Li C, Lin L, Pan Y, Wang H, Zhao J & Zhang D. Assessment of alveolar bone status in middle aged Chinese (40-59 Years) with chronic periodontitis—using CBCT. PLoS One 2015;10(10): e0139553.
- Zhang X, Li Y, Ge Z, Zhao H, Miao L & Pan Y. The dimension and morphology of alveolar bone at maxillary anterior teeth in periodontitis: a retrospective analysis—using CBCT. Int J Oral Sci 2020;12(1): 1-9.
- Scarfe WC, & Angelopoulos C. Maxillofacial cone beam computed tomography: principles, techniques and clinical applications. Springer Book 2018; 115-189. ISBN:978-3-319-62059-6 (ed.1).
- Kamburoğlu K, Schulze D, Murat S, Melo S L S, Li Z, Bornstein, M M & Scarfe W C (2018). CBCT imaging of sinonasal disease. In Maxillofacial Cone Beam Computed Tomography Springer, Cham Book 2018;1155-1205.
- Fokas G, Vaughn V M, Scarfe WC & Bornstein MM. Accuracy of linear measurements on CBCT images related to presurgical implant treatment planning: A systematic review. Clin Oral Implants Resn 2018;29: 393-415.
- Cheng X. A 3d approach in quantification of the alveolar bone changes after dental implant placement based on CBCT images. Degree of Doctor of Philosophy Submitted to Bart's and The London School of Medicine and Dentistry, Queen Mary, University of London 2016.
- Cetmili H, Tassoker M & Sener S. Comparison of cone-beam computed tomography with bitewing radiography for detection of periodontal bone loss and assessment of effects of different voxel resolutions: an in vitro study. Oral radiol 2019;35(2):177-183.
- Sharma H, Dahiya P, Gupta R, Kumar M, Melwani S R & Kachroo L. Comparison of conventional and digital radiographic techniques for the assessment of alveolar bone in periodontal disease. Indian J Dent Sci 2019;11(3):138.
- Bagis N, Kolsuz ME, Kursun S, Orhan K. Comparison of intraoral radiography and cone-beam computed tomography for the detection of periodontal defects: an in vitro study. BMC Oral Health 2015;15(1):64.
- Song D, Shujaat S, de Faria Vasconcelos K, Huang Y, Politis C, Lambrichts I & Jacobs R. Diagnostic accuracy of CBCT versus intraoral imaging for assessment of peri- implant bone defects. BMC Med Imaging 2021;21(1):1-8.
- Almeida VC, Pinheiro LR, Salineiro FC S, Mendes FM, Neto JBC, Cavalcanti MGP & Pannuti CM. Performance of cone beam computed tomography and conventional intraoral radiographs in detecting interproximal alveolar bone lesions: a study in pig mandibles. BMC oral health 2017;17(1):1-8.
- Vasconcelos KF, Evangelista KM, Rodrigues CD, Estrela C, de Sousa TO, Silva MAG. Detection of periodontal bone loss using cone beam CT and intraoral radiography. DentomaxillofacRadiol 2012;41:64–69.